



Cite this: *Environ. Sci.: Processes Impacts*, 2025, **27**, 1573

## Oxidant concentrations and photochemistry in a vehicle cabin

Pedro A. F. Souza, <sup>a</sup> Corey R. Kroptavich, <sup>b</sup> Shan Zhou, <sup>c</sup> and Tara F. Kahan, <sup>ab</sup>

Indoor air quality (IAQ) in vehicles can be important to people's health, especially for those whose occupations require them to spend extensive time in vehicles. To date, research on vehicle IAQ has primarily focused on direct emissions as opposed to chemistry happening in vehicle cabins. In this work, we conducted time-resolved measurements of the oxidants and oxidant precursors ozone ( $O_3$ ), nitric oxide (NO), nitrogen dioxide ( $NO_2$ ), and nitrous acid (HONO) inside the cabin of a 2012 Toyota Rav4 under varying ventilation conditions (*i.e.*, car off, car on with passive ventilation, car on with mechanical ventilation *via* the recirculating fan, and car on with mechanical ventilation *via* the direct fan). Ozone levels inside the vehicle were significantly lower than outdoors under most conditions, and were approximately half the outdoor levels when the direct fan was in operation. Nitric oxide and  $NO_2$  concentrations were very low both inside the vehicle and outdoors. Nitrous acid levels in the vehicle were lower than reported values in other indoor environments, though much higher than expected outdoor levels. We also investigated the potential for photochemical production of radicals in the vehicle. Time- and wavelength-resolved solar irradiance spectra were collected, and steady state hydroxyl radical (OH) and nitrate radical ( $NO_3$ ) concentrations were calculated. Steady state OH concentrations were predicted to be similar to those in air masses in residences illuminated by sunlight, suggesting the importance of HONO photolysis in vehicles. Conversely, nitrate radicals ( $NO_3$ ) were not considered significant indoor oxidants in our study due to rapid titration by NO. Overall, our findings emphasize the importance of both air exchange and photochemistry in shaping the composition of air inside vehicles.

Received 29th May 2024

Accepted 8th July 2024

DOI: 10.1039/d4em00319e

rsc.li/espi

### Environmental significance

Understanding indoor air quality (IAQ) within vehicle cabins is critical for public health, particularly for individuals who spend extensive periods commuting or driving as part of their occupation. Our findings reveal that, similar to residential environments, the levels of key pollutants such as ozone ( $O_3$ ), nitrogen oxides ( $NO_x$ ), and nitrous acid (HONO) are influenced by ventilation rates and, consequently, the quality of outdoor air. This study demonstrates that photolysis of HONO can generate hydroxyl radicals (OH) in concentrations comparable to those reported in other sunlit indoor environments. These results highlight the importance of considering both air exchange and photochemistry when assessing IAQ in vehicles. These results may inform the development of strategies to mitigate exposure to harmful pollutants in vehicles.

## Introduction

Indoor air quality (IAQ) is important to human health, given that most people spend the vast majority of their lives indoors. While most of this time is spent in buildings (Americans spend an average of 69% of their lives in residences and 18% in non-residential buildings), a small but significant fraction of time is

spent in vehicles.<sup>1</sup> For North Americans, the average fraction is 6%, and for many people whose occupations centre around driving, the fraction is much greater. Developing an understanding of the composition of air in vehicles, and the factors that affect air quality there, is therefore important to promoting good health.

Air quality in vehicle cabins has been studied from a number of perspectives. The most common approach has been to measure concentrations of species emitted from vehicle exhaust or interior materials, including carbon monoxide (CO), particulate matter (PM), and volatile organic compounds (VOCs).<sup>2-7</sup> Factors including type of fuel, use of air fresheners, interior material type, and vehicle age have been reported to affect VOC mixing ratios.<sup>5,6</sup> On the other hand, infiltration of outdoor air due to open windows or mechanical ventilation were reported to

<sup>a</sup>Department of Chemistry, University of Saskatchewan, Saskatoon, SK, Canada.  
E-mail: tara.kahan@usask.ca

<sup>b</sup>Department of Chemistry, Syracuse University, Syracuse, NY, USA

<sup>c</sup>Department of Civil and Environmental Engineering, Rice University, Houston, TX, USA

† Currently at School of Engineering, Eastern Institute of Technology, Ningbo, China.



have the greatest effects on PM and CO concentrations in the absence of an internal source.<sup>3,4</sup> While studies to date have focused primarily on direct emissions, we hypothesize that chemistry may be important to IAQ in vehicle cabins, just as it can be in residential and non-residential buildings under some conditions.

Oxidizing capacity outdoors is generally dominated by hydroxyl radicals (OH) during the day and ozone (O<sub>3</sub>) and nitrate radicals (NO<sub>3</sub>) at night. Indoors, the lack of high energy photons makes O<sub>3</sub> photolysis (the primary source of OH) insignificant, and high nitric oxide (NO) and low O<sub>3</sub> concentrations means that NO<sub>3</sub> has only been detected indoors under highly contrived or unusual conditions, such as when both a gas stove and an O<sub>3</sub> generator are running simultaneously or in an athletic complex with high ventilation rates and low levels of NO<sub>3</sub> sinks.<sup>8–11</sup> Ozone is therefore often considered to be the most important indoor oxidant, but its levels depend strongly on the rate of exchange between indoor and outdoor air. In commercial buildings with high air change rates (ACR), O<sub>3</sub> concentrations can be up to 85% of those outdoors, while in residential buildings with low ACR, O<sub>3</sub> levels lower than 1 ppbv have been reported.<sup>12,13</sup> Ozone itself is therefore only occasionally an important indoor oxidant.

In indoor environments with high ACR and correspondingly high O<sub>3</sub> concentrations, OH can be generated by ozone–alkene reactions. The OH steady state concentrations predicted and measured under these conditions is 1–2 orders of magnitude lower than those measured outside during the day.<sup>14–17</sup> However, OH can also be formed indoors *via* nitrous acid (HONO) photolysis. While the high energy photons required to convert O<sub>3</sub> to OH ( $\lambda < 320$  nm) are attenuated indoors by windows, HONO photolyses at wavelengths as long as 405 nm, producing OH with a unity quantum yield.<sup>18–21</sup> Given that most windows used in buildings transmit light at wavelengths longer than 330–340 nm, HONO photolysis has been shown experimentally and theoretically to produce OH in concentrations of  $\sim 10^6$ – $10^7$  molecules cm<sup>−3</sup> in indoor air volumes illuminated by direct sunlight.<sup>15,18,22–24</sup> Some artificial lights, such as fluorescent tubes, can also generate significant OH concentrations, although the volume of air in which this chemistry occurs is relatively small given the rapid decay of irradiance with distance from the source.<sup>18,25</sup>

Ozone can be readily measured indoors, but OH and NO<sub>3</sub> are much more challenging due to expected low concentrations, the need for highly specialized instrumentation, and logistical difficulties associated with operating the instruments in occupied indoor spaces. Indoor OH and NO<sub>3</sub> concentrations are therefore often estimated using steady state calculations, with the assumptions that all important oxidant production and loss mechanisms are included, and that reactant concentrations are accurate. Eqn (1) shows a generic equation for a steady state calculation:

$$[\text{oxidant}]_{\text{ss}} = \frac{\sum \text{rate}_f}{\sum k'_i} \quad (1)$$

where [oxidant]<sub>ss</sub> is the concentration of the oxidant (or other reactive intermediate) at steady state,  $\sum \text{rate}_f$  is the sum of all

rates of production of the oxidant, and  $\sum k'_i$  is the sum of all first-order and pseudo-first-order rate constants for oxidant loss processes. Eqn (2) and (3) show expressions for indoor OH and NO<sub>3</sub> steady state concentrations, respectively. A more thorough discussion of indoor steady state calculations is provided in Kahan *et al.*<sup>26</sup>

$$[\text{OH}]_{\text{ss}} =$$

$$\frac{J_{\text{HONO}}[\text{HONO}] + \sum k_{\text{O}_3-\text{alkene}}[\text{alkene}][\text{O}_3]\Phi_{\text{OH}}}{\text{ACR} + k_{\text{OH-NO}}[\text{NO}] + k_{\text{OH-NO}_2}[\text{NO}_2] + k_{\text{OH-HONO}}[\text{HONO}]} \quad (2)$$

$$[\text{NO}_3]_{\text{ss}} =$$

$$\frac{k_{\text{O}_3-\text{NO}_2}[\text{O}_3][\text{NO}_2]}{\text{ACR} + J_{\text{NO}_3} + k_{\text{NO}_3-\text{VOC}}[\text{VOC}] + k_{\text{NO}_3-\text{NO}}[\text{NO}]} \quad (3)$$

J<sub>HONO</sub> is the HONO photolysis rate constant, and  $\sum k_{\text{O}_3-\text{alkene}}$  is the sum of important 2<sup>nd</sup> order rate constants for OH formation from ozone–alkene reactions.  $k_{\text{OH-NO}}$  and  $k_{\text{OH-NO}_2}$  are the 2<sup>nd</sup> order rate constants for OH reacting with NO and nitrogen dioxide (NO<sub>2</sub>), respectively.  $k_{\text{O}_3-\text{NO}_2}$  is the 2<sup>nd</sup> order rate constant for O<sub>3</sub> with NO<sub>2</sub>,  $J_{\text{NO}_3}$  is the NO<sub>3</sub> photolysis rate constant, and  $k_{\text{NO}_3-\text{VOC}}$  and  $k_{\text{NO}_3-\text{NO}}$  are the 2<sup>nd</sup> order rate constants for NO<sub>3</sub> with VOCs and NO, respectively. Loss of OH to VOCs is not considered in eqn (2), as we assume that the HO<sub>2</sub> formed from this reaction will react quickly with NO to regenerate OH.<sup>17,22</sup> As long as the concentrations of all listed reactants are known, along with wavelength-resolved photon fluxes or  $J_{\text{HONO}}$  and  $J_{\text{NO}_3}$ , these equations can estimate steady state OH and NO<sub>3</sub> concentrations. Although there are almost no measurements of these radicals indoors, we have shown that OH concentrations predicted using this method in a classroom in France are in good agreement with measurements.<sup>24</sup> Few reports of relevant reactant concentrations in vehicles exist, and, to our knowledge, wavelength-resolved photon fluxes have not been reported in vehicle cabins. Existing reports include: ozone concentrations of 11.7 ppbv,<sup>27</sup> NO<sub>2</sub> concentrations ranging from 21–43 ppbv,<sup>27,28</sup> and HONO concentrations ranging from  $\sim 9$ –29 ppbv.<sup>28</sup> In this work, we measured concentrations of O<sub>3</sub>, NO, NO<sub>2</sub>, and HONO in the cabin of a personal vehicle, along with wavelength-resolved solar irradiance, to improve our understanding of the oxidizing capacity inside personal vehicle cabins.

## Methods

Five separate continuous measurement campaigns were conducted: September 30, 2018 (6 h 30 min), October 14, 2018 (5 h 30 min), December 16, 2018 (7 h 30 min), May 17–18, 2019 (36 h 0 min), and August 16, 2020 (6 h 30 min). Each campaign was conducted in a parking lot at Syracuse University that was surrounded by residential streets on 3 sides. The vehicle used for the experiments was a 2012 Toyota Rav4 with a cloth interior. The vehicle was kept motionless throughout the measurement period and in-cabin analyte measurements were made under four different conditions: car off (car off), car on with passive ventilation (fan off), car on with mechanical ventilation *via* the



recirculating fan (recirculation), and car on with mechanical ventilation *via* the direct fan (direct fan). Outdoor measurements were acquired in between each tested setting. The vehicle was used by its owner, primarily for in-city commuting, in between campaigns.

The time resolved mixing ratios of O<sub>3</sub>, NO, NO<sub>2</sub>, and HONO were measured using a custom-built mobile analytical laboratory (Mobile Indoor Laboratory for Oxidative Species, MILOS). Ozone was quantified using an Ecotech Serinus 10 UV photometric analyzer with an accuracy of 0.5 ppbv. Nitric oxide, NO<sub>2</sub>, and HONO were quantified using an Ecotech Serinus 40 O<sub>3</sub>-based chemiluminescence analyzer with an accuracy of 0.4 ppbv. The analyzer converts both HONO and NO<sub>2</sub> to NO, and reports the sum of these two species as NO<sub>2</sub>. We determined speciated concentrations of NO<sub>2</sub> and HONO *via* a difference method, which is described in detail elsewhere.<sup>29,30</sup> In short, the inlet line was split in two, and a Teflon solenoid valve was used to alternate between the two lines every 5 minutes. One line led directly to the Serinus 40, while the other first passed through a denuder coated with sodium carbonate to remove gaseous acids, including HONO. By subtracting the NO<sub>2</sub> mixing ratio reported when the collected air passed through the denuder from the mixing ratio reported when it went straight to the analyzer, we were able to quantify both HONO and NO<sub>2</sub>.

Calibrations for the two analyzers were performed before and after the testing periods. The calibrations used a dilution calibrator and ozone generator (Ecotech GasCal 1100) and an NO cylinder (19.8 ppmv in N<sub>2</sub>, analytical uncertainty of 5%). The 30 s limits of detection (LODs) for the analytes were determined as 3 times the standard deviations ( $3\sigma$ ) of the corresponding signals in zero air. The LODs for O<sub>3</sub>, NO, NO<sub>2</sub>, and  $\Sigma$ (NO<sub>2</sub> + HONO) were 0.65, 1.2, 1.5, and 1.5 ppbv respectively. The 5 min LOD of HONO was calculated as 0.7 ppbv from the standard deviation of the subtraction of NO<sub>2</sub> from  $\Sigma$ (NO<sub>2</sub> + HONO). The quality control of the system followed the same method outlined in Zhou *et al.*<sup>29</sup>

MILOS was stationed inside the university building in the stairwell nearest the parking lot in which the vehicle was located. The Teflon sampling inlet was placed inside the vehicle cabin through the driver side window and secured to the steering wheel. The window was opened wide enough for only the inlet to enter and was then sealed using parafilm. The inlet included a *T*-valve to allow switching between sampling air inside and outside of the vehicle. The outdoor inlet was placed on the hood of the vehicle in front of the driver. Exhaust measurements were conducted by suspending the outdoor inlet in the path of the exhaust exiting through the tailpipe.

Air change rates were measured within the vehicle under each ventilation setting. Approximately 20 g of dry ice was broken up and scattered throughout the cabin and allowed to sublimate, and CO<sub>2</sub> mixing ratios were recorded at 30 s intervals by a TSI IAQ7545. The CO<sub>2</sub> was measured over 2 h periods for all settings except the direct fan where 30 min was determined to be sufficient for CO<sub>2</sub> levels to return to background levels. The collected data was analyzed and a quantile regression was used to determine the air change rate. A detailed description of the

analysis is provided by Zhou *et al.*<sup>29</sup> None of the air change tests occurred while an occupant was present in the vehicle.

Wavelength-resolved solar irradiance was collected through vehicle windows using a calibrated Ocean Optics USB4000 spectrometer coupled to a 1 m fiber optic cable and a cosine corrector. Average spectral irradiances were collected and photon fluxes were estimated using the method reported by Kowal *et al.*<sup>18</sup> On May 18, irradiance was acquired through the closed front passenger window of the vehicle with 1 min resolution over a period of 6 hours. Single irradiance measurements were also acquired in 3 additional vehicles with windows opened and closed to determine the wavelength-resolved transmittance of the windows, as described in ref. 23 for windows in buildings.

## Results

### Reactant mixing ratios and air change rates

Air change rate is a key factor affecting indoor air composition. For example, ozone levels in commercial buildings with high ACR ( $>5\text{ h}^{-1}$ ) can reach up to 85% of outdoor levels,<sup>13</sup> while levels in residential buildings with low ACR ( $\sim 0.5\text{ h}^{-1}$ ) are generally below 5 ppbv, and often below 1 ppbv.<sup>31</sup> Other species, such as NO, are often emitted directly indoors (*e.g.*, *via* combustion), with negative concentration dependences on ACR.<sup>32,33</sup> Table 1 lists ACR measured in the test vehicle under different conditions, as well as reported ACR in stationary vehicles for models spanning from 2005 to 2010.<sup>34,35</sup> Air change rates in the parked vehicle were the same whether the engine was on or off ( $0.4\text{ h}^{-1}$ ) when no fans were running. This is similar to ACRs reported in residences with closed doors and windows ( $0.5\text{ h}^{-1}$ ).<sup>36</sup> The use of the recirculating fan increases the measured ACR by a factor of  $\sim 3.8$ , likely due to a shift in the internal pressure caused by the increased air flow velocity in the cabin. Air change rates ranging from 0.1 to  $2.9\text{ h}^{-1}$  have previously been reported for stationary vehicles, with older models having higher ACR due to poorer air tightness.<sup>34,35,37</sup> With the direct fan, which pulls outdoor air into the car, we measured very large ACRs ( $\sim 54\text{ h}^{-1}$ ). This agrees with reported ACR measurements ranging from 23 to  $97\text{ h}^{-1}$  in other 2010 Toyota model vehicles.<sup>35</sup>

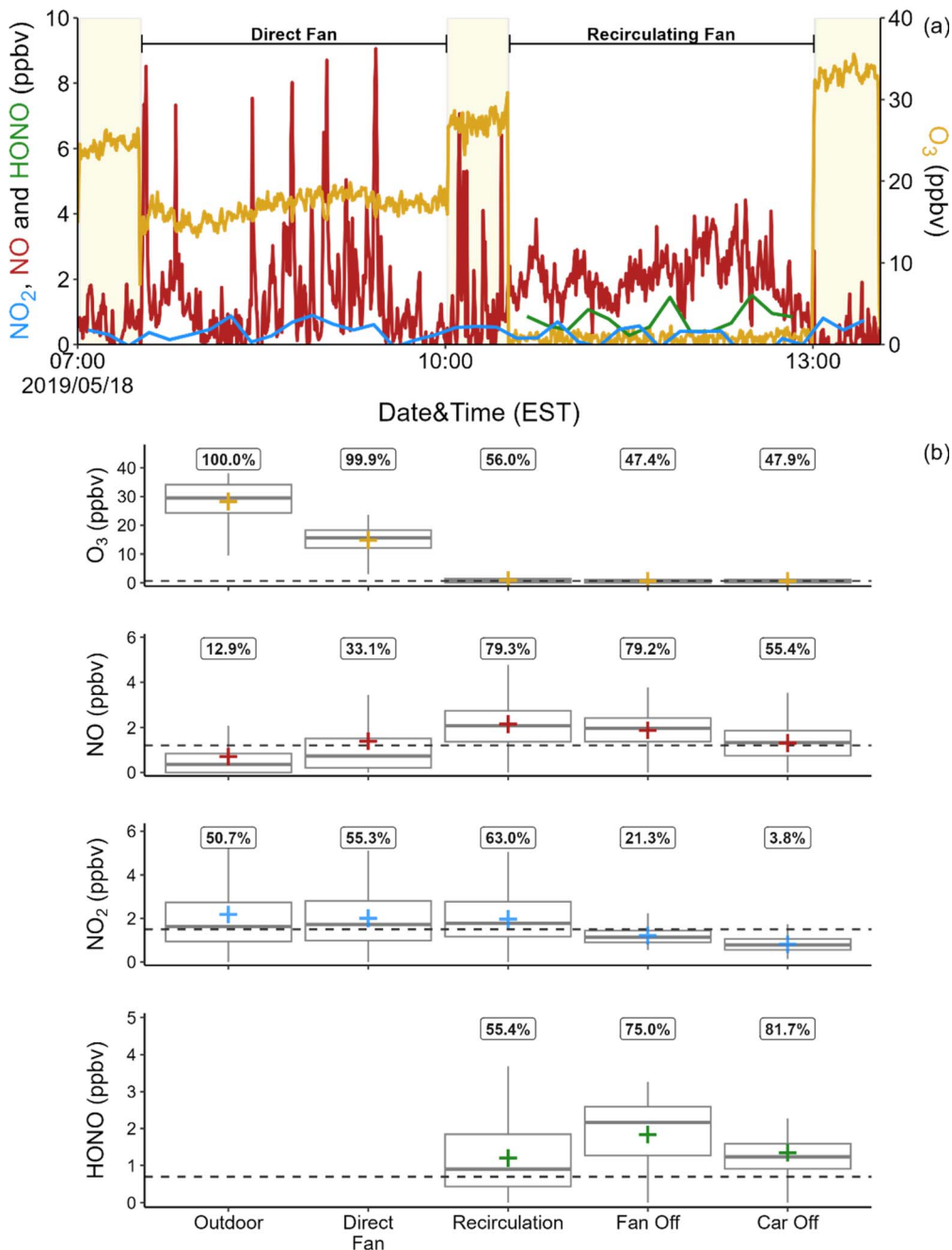
Fig. 1a shows a 7 hours time series from a sampling period on May 18, 2019. This period was selected to illustrate analyte

Table 1 Average air change rates in vehicles under different ventilation conditions

Condition	Air change rate ( $\text{h}^{-1}$ )	
	This work	Literature <sup>a</sup>
Car off	$0.35 \pm 0.14\ (N = 6)$	$0.74 \pm 0.62\ (N = 7)$
Fan off	$0.38 \pm 0.11\ (N = 6)$	—
Recirculation	$1.50 \pm 0.30\ (N = 7)$	$1.65 \pm 1.36\ (N = 11)$
Direct fan	$54.3 \pm 21.9\ (N = 6)$	$61.5 \pm 32.6\ (N = 15)$

<sup>a</sup> Assessed from literature describing vehicles built between 2005 and 2010.<sup>34,35</sup> Values stated are averages from the mean described ACR for each condition.





**Fig. 1** (a) Representative time series for NO, NO<sub>2</sub>, HONO, and O<sub>3</sub> over 7 hours of measurements. Light yellow shaded regions represent outdoor measurements. (b) Box-and-whiskers plot for analyte concentrations under indoor and outdoor conditions. Box plots display quartile values and medians. Whiskers extend to the minimum and maximum values within 1.5 times the interquartile range. Crosses represent the mean value for each condition. Horizontal dashed lines represent the LOD for each species, and percentages above the violin plots represent the fraction of measurements above the LOD. Nitrous acid concentrations under outdoor and direct fan conditions are not reported due to a sampling artefact.

levels with the direct fan on (pulling in outdoor air) and off. Oxidant levels over the entire campaign period are summarized in Fig. 1b. Ozone levels were consistently much higher outdoors than inside the vehicle. Outdoor O<sub>3</sub> levels varied diurnally, with peak levels of ~38 ppbv around 10 a.m. and minimum values of ~5 ppbv at night. Ozone in the vehicle was below the LOD (0.65 ppbv) for approximately 49% of all measurements for all conditions excluding direct fan (herein referred to as sealed

conditions), with a mean of  $0.78 \pm 0.75$  ppbv. When the direct fan was on, mean indoor O<sub>3</sub> levels were  $14.8 \pm 4.6$  ppbv, approximately 50% of the mean outdoor levels.

As shown in Fig. 1b, mean NO concentrations in the vehicle under sealed conditions were  $1.75 \pm 1.01$  ppbv, while levels were generally below the LOD of 1.2 ppbv outdoors and under direct fan conditions. However, sharp spikes (lasting ~3 min and ranging in concentration from 4–57 ppbv) were



occasionally observed outdoors and under direct fan conditions, as illustrated in Fig. 1a. These spikes were not observed under any of the sealed conditions. Fourteen spikes were observed under direct fan conditions and 9 were observed while sampling outdoor air. Exhaust from the test vehicle could be the source of these spikes; NO mixing ratios of  $272 \pm 92$  ppbv were measured with the inlet placed inside the vehicle's exhaust pipe. However, the cumulative duration of these spikes was only  $\sim 1$  h, while total outdoor and direct fan sampling time exceeded 24 h, so the overall impact of exhaust from the vehicle on NO mixing ratios within the vehicle and outside of the vehicle close to the passenger window is minor. We also measured NO levels inside the vehicle under direct fan conditions while another vehicle drove by the test vehicle ( $\sim 2$  m separation, 5 passes). No spikes in NO were observed during these experiments. It is possible that at least some of the observed spikes are due to sources such as traffic on nearby roads. The NO mixing ratio showed a gradual increase over time under the recirculating fan condition in 4 of 6 of sampling periods (average rate of increase =  $2.4 \pm 1.2$  ppbv  $h^{-1}$ ). The internal temperature of the ventilation system isn't high enough to be a major source of thermal NO<sub>x</sub>. It is possible that the observed increase in NO is a byproduct of engine combustion.

As shown in Fig. 1b, mean NO<sub>2</sub> levels were frequently below the LOD of 1.5 ppbv under all vehicle conditions. Mixing ratios were also low outdoors, with a mean of  $2.2 \pm 2.0$  ppbv, and with only 51% of measurements above the LOD. A previous study reported NO<sub>2</sub> concentrations in a vehicle of  $\sim 33$  ppbv, but outdoor NO<sub>2</sub> levels were also much higher in that study.<sup>28</sup> Similarly, we previously reported a mean NO<sub>2</sub> mixing ratio of 2.0 ppbv in a house in Syracuse; outdoor levels during those measurements were estimated to be approximately 5.2 ppbv.<sup>26</sup> Common sources of indoor NO<sub>2</sub> include transport from outdoors, reaction between O<sub>3</sub> and NO, and direct emission from combustion. It is likely that the primary source of indoor NO<sub>2</sub> in the vehicle is infiltration of outdoor air.

Mean HONO mixing ratios under sealed conditions were  $1.43 \pm 0.99$  ppbv. This is lower than the reported values of 4–5 ppbv in residential and non-residential buildings,<sup>29,38,39</sup> and is also much lower than the sole reported level in a vehicle of 9–29 ppbv.<sup>28</sup> The difference between levels measured in the two vehicles is likely explained by the much higher NO<sub>2</sub> levels inside the vehicle as well as outdoors in the previous study (21–43 ppbv NO<sub>2</sub>). Interestingly, HONO : NO<sub>2</sub> ratios inside the vehicle under sealed conditions were much lower in the previous study than in this work (0.4 vs. 1.0). We previously reported HONO : NO<sub>2</sub> ratios ranging from 1.1–2.2 in an occupied residence,<sup>29</sup> similar to the mean ratio observed in this work.

Due to low analyte concentrations outdoors (NO, NO<sub>2</sub>) or in the vehicle (NO<sub>2</sub>, O<sub>3</sub> under sealed conditions), we do not report indoor-outdoor ratios (*I/O*). The exception is O<sub>3</sub> under direct fan conditions, where we determined a mean *I/O* of 0.57. This is consistent with high O<sub>3</sub> concentrations reported in non-residential buildings with high ACR or in residential buildings with windows open, compared to levels below 5 ppbv reported in residences with low ACR when doors and windows are closed.<sup>29,40</sup>

## Photochemistry

Photolysis of HONO has been suggested to be an important indoor OH source.<sup>15,41</sup> While windows often attenuate sunlight completely at wavelengths shorter than 330–340 nm, HONO remains photo-labile at wavelengths as long as 405 nm,<sup>19</sup> and photochemically-formed OH has been reported in sunlit rooms.<sup>15,22,24,42</sup> Given the large surface area of windows in cars, it is possible that OH could also be photochemically formed in such indoor environments. We measured solar irradiance in several vehicles to predict OH steady state concentrations in sunlit vehicles. Fig. 2a shows transmittance of the driver side window of three vehicles. Transmittance was similar in all three windows despite differences in make and age of the vehicles. The wavelength-resolved transmittance profile of each window was characterized by a broad hump centered around 370 nm. This feature is not generally observed in windows in buildings, as seen in the average transmittance profile of windows in single-family residences on the same plot. However, there is significant variability in the wavelength-resolved transmittance of windows in buildings. The transmittance of the 3 vehicle windows is within this uncertainty at wavelengths between 340 and 400 nm. Fig. 2b shows transmittance of four different windows in a 2013 Honda CRV. Driver and front passenger

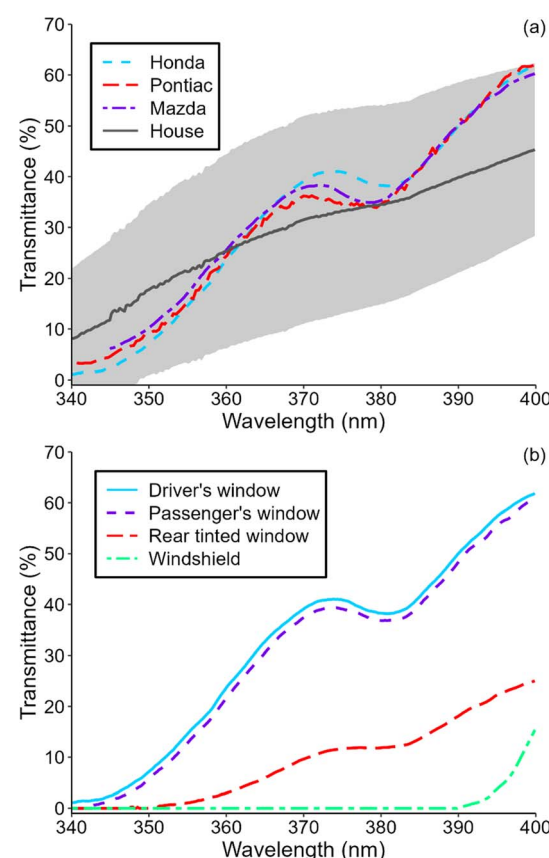


Fig. 2 (a) Transmittance of driver-side windows in a 2013 Honda CRV, a 2006 Pontiac G6 sedan, and a 2016 Mazda 3 hatchback. Average transmittance of 13 windows in 13 single-family residences (standard deviation in shaded grey) is also shown for reference.<sup>23</sup> (b) Transmittance of various windows in the Honda CRV.



windows had very similar transmittance, but the rear passenger window, which was tinted, had much lower transmittance. The windshield, on the other hand, attenuated sunlight almost completely at wavelengths shorter than 390 nm since it is made from laminated glass.<sup>43</sup>

Indoor solar photon fluxes vary throughout the day, with minimum values at night or in spaces without windows. The time at which photon fluxes are highest depends both on the intensity of the sun (which generally peaks close to noon), and the orientation of windows.<sup>23</sup> For example, maximum indoor solar intensity in a classroom in France was observed at 6 p.m., when sunlight entered windows directly.<sup>44</sup> Fig. 3 shows a time-series for the wavelength-resolved photon flux within the parked Toyota, measured near the front passenger window. Photon flux within the vehicle fluctuated over time due to influences such as intermittent cloud cover in the morning and around noon. The maximum flux was observed at 11:31, which correlates with the solar maximum on that day. The sharp cut off of light at 13:50 corresponds to the time when the sun moved behind a nearby building and put the vehicle in the building's shadow.

We used the photon flux and measured NO, NO<sub>2</sub>, and HONO concentrations to estimate steady state OH number densities during the period of maximum solar intensity in the vehicle (11:31 a.m.) using eqn (2). Ozone photolysis was not considered in the steady state calculations due to attenuation of sunlight by the glass at wavelengths shorter than  $\sim 340$  nm, but we did consider ozone–alkene reactions under direct fan conditions. Table 2 shows predicted [OH]<sub>ss</sub> for several indoor locations including a vehicle (sealed conditions), a home, and a classroom. Nitrous acid photolysis rate constants when sunlight is filtered through side windows of a vehicle are similar to those measured in several office and laboratory buildings and in a residence,<sup>15,18,29,48,50,51</sup> but calculated OH production rates are lower than in buildings due to lower HONO mixing ratios measured in the vehicle. Despite lower calculated OH

production rates in vehicles than in buildings, we predict steady state OH concentrations in vehicles to be similar to those in residences and higher than those in non-residential buildings due to lower concentrations of OH sinks in vehicles. These concentrations are also similar to those measured and predicted in a variety of residential and non-residential buildings under sunlit conditions.<sup>32,41,48,50</sup> The OH steady state concentrations predicted in an illuminated vehicle are similar to those measured outdoors in cities, and we conclude that HONO photolysis can be an important OH source in vehicles under sealed conditions. We note that the steady state OH concentrations listed in Table 2 are subject to large uncertainty. There are few measurements of wavelength-resolved UV irradiance in buildings (and therefore few calculated HONO photolysis rate constants), and to our knowledge, our measurements are the first performed in vehicles. As discussed above, one previous measurement of HONO in vehicles has been reported – the average level in that study was  $\sim 14$  ppbv, nearly ten times higher than the 1.4 ppbv measured in this work.<sup>28</sup> Despite the higher predicted OH formation rates, we predict similar or lower [OH]<sub>ss</sub> under those conditions, as NO<sub>2</sub> concentrations (and likely NO concentrations as well, although they were not reported) were also much higher, resulting in a correspondingly elevated loss term.

As previously mentioned, HONO levels were not quantified under direct fan conditions, but reported outdoor daytime concentrations in North America range from 9–150 pptv.<sup>52,53</sup> With these low HONO concentrations, we predict [OH]<sub>ss</sub> of  $0.52\text{--}8.4 \times 10^5$  molecules  $\text{cm}^{-3}$  when the direct fan is on. However, with increased ozone mixing ratios (averaging 14.8 ppbv with the direct fan on), alkene ozonolysis could be a significant OH source. Using reported alkene concentrations of 4–50 ppbv in vehicles,<sup>5,54</sup> and assuming that isoprene is the dominant alkene,<sup>55,56</sup> we estimate [OH]<sub>ss</sub> due to alkene ozonolysis of  $0.15\text{--}1.7 \times 10^6$  molecule  $\text{cm}^{-3}$ , and a total [OH]<sub>ss</sub> (from both HONO photolysis and alkene ozonolysis) of up to  $2.5 \times 10^6$

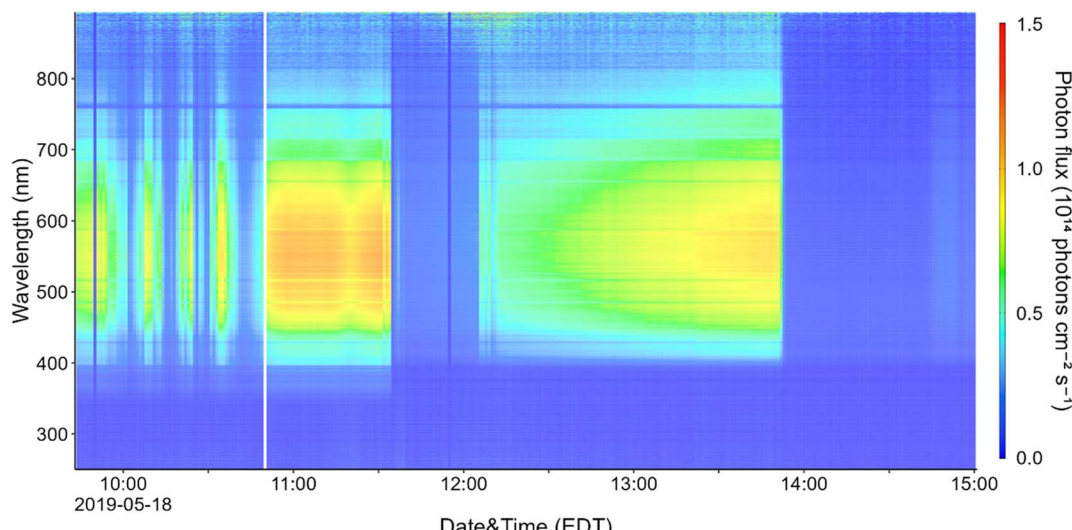


Fig. 3 Time series of photon flux taken inside the Toyota on May 18, 2019. Data was not available for a short period at 10:50 a.m.; this is reflected by the white pixels at all wavelengths at that time.



**Table 2** Photolytic HONO rate constants and estimated steady state OH concentrations in the vehicle under sealed in-cabin conditions (vehicle on, off, and recirculating fan) and in other indoor environments. Rate constants and mixing ratios from multiple literature sources are mean values

Environment	$J_{\text{HONO}} (10^{-4} \text{ s}^{-1})$	Reactant mixing ratios (ppbv)			OH production rate (molecules $\text{cm}^{-3} \text{ s}^{-1}$ )	$[\text{OH}]_{\text{ss}} (\text{molecules } \text{cm}^{-3})$
		HONO	NO	$\text{NO}_2$		
Vehicle	Side front windows	2.1 <sup>a</sup>	1.43 <sup>a</sup>	1.75 <sup>a</sup>	7.48 $\times 10^6$	7.39 $\times 10^6$
	Rear tinted windows	0.21 <sup>a</sup>			7.62 $\times 10^5$	7.53 $\times 10^5$
	Windshield	0.0013 <sup>a</sup>			4.52 $\times 10^3$	4.47 $\times 10^3$
Houses	Unperturbed	2.8 <sup>23</sup>	4.34 <sup>29,38,44-46</sup>	4.11 <sup>29,46,47</sup>	5.54 <sup>29,46,47</sup>	2.01 $\times 10^7$
	Cooking		22.9 <sup>29,48,49</sup>	165 <sup>29,49</sup>	95.3 <sup>29,49</sup>	1.06 $\times 10^8$
Classrooms		1.8 <sup>15,18,48,50,51</sup>	4.75 <sup>15,48</sup>	2.17 <sup>15,29,32</sup>	12.4 <sup>15,48</sup>	2.18 $\times 10^7$

<sup>a</sup> This work.

molecule  $\text{cm}^{-3}$ . These predicted levels would increase in locations with higher outdoor ozone concentrations. These estimates are highly uncertain due to the lack of alkene and HONO measurements in vehicles under direct fan conditions, but they suggest that OH concentrations in vehicles may be high enough to effect oxidation even when ventilation rates are high, such as when the direct fan is operating or windows are open. We note that when windows are open,  $\text{O}_3$  photolysis will likely be the most important OH source in vehicles illuminated by sunlight.

While nitrate radicals ( $\text{NO}_3$ ) are generally present at negligibly low levels indoors (e.g., ref. 29, 57 and 58), we have hypothesized that they could be important in indoor environments with high ACR, due to high expected levels of  $\text{O}_3$  and low NO.<sup>11</sup> This hypothesis is supported by recent observations of  $\text{NO}_3$  reactivity in an athletic centre with high ACR.<sup>11</sup> We therefore estimated steady state  $\text{NO}_3$  concentrations in the vehicle under direct fan conditions using a simplified version of eqn (3). Considering reaction with NO as the only important  $\text{NO}_3$  sink provided an upper limit for  $[\text{NO}_3]_{\text{ss}}$  of  $6.57 \times 10^5$  molecules  $\text{cm}^{-3}$  ( $\sim 0.03$  pptv). The lifetime of  $\text{NO}_3$  toward reaction with NO in the vehicle was estimated to be  $\sim 1$  s, while lifetimes toward photolysis and air change were on the order of 1 minute (52 and 66 s, respectively). Together, photolysis and air change accounted for only 4% of total loss. We did not consider loss to reactions with VOCs in our calculations due to the large uncertainties surrounding VOC concentrations and speciation in vehicles, so, as noted above, the estimated steady state concentrations are upper limits. While including a VOC loss term might change the predicted  $\text{NO}_3$  steady-state concentration, it will not change our conclusion that  $\text{NO}_3$  was not an important oxidant in this vehicle. It is possible that  $\text{NO}_3$  could contribute to oxidation capacity in vehicles if NO concentrations are low enough (e.g., if air masses entering the vehicle are aged, with  $\text{NO}_2$  levels greatly exceeding NO levels), as was the case in the study performed in the athletic centre.<sup>11</sup>

## Environmental implications

Air composition and quality inside vehicle cabins depends on many factors, including outdoor air quality and emissions from interior materials. A number of species that affect IAQ, such as

VOCs, CO,  $\text{CO}_2$ , and  $\text{PM}_{2.5}$ , have been quantified in personal and commercial vehicles. This work adds to the existing literature by providing insight into the capacity for chemistry to occur in vehicles, and illustrates the importance of both air exchange and photochemistry on indoor air composition. Our results suggest that the ventilation conditions within the vehicle, in addition to outdoor analyte concentrations, will determine indoor concentrations. While  $\text{NO}_x$  and HONO concentrations were lower in the vehicle than in a residential and non-residential building in the same city,<sup>32</sup> this is very likely due to outdoor concentrations of these analytes also being lower during the sampling periods. We also note that the vehicle was in a parking lot. Air quality is well known to be poorer on roads – especially busy roads – than in surrounding areas. Therefore, it is likely that  $\text{NO}_x$  and HONO levels in the vehicle would have been higher during commutes. Future measurements of oxidants and oxidant precursors in vehicles under normal use would be beneficial.

This study also shows that photochemistry can increase indoor oxidizing capacity to levels similar to those observed in cities outdoors during the day. While mixing ratios of HONO, the primary photochemical OH source indoors, were lower in the sealed vehicle cabin than in residential and non-residential buildings, we predict similar OH concentrations under sunlit conditions due to lower concentrations of OH sinks (NO and  $\text{NO}_2$ ) in the vehicle. We also note that a greater fraction of the interior volume of the vehicle will be illuminated at any given time than in most buildings due to the larger relative surface area covered by windows, making photochemistry more likely to happen in vehicles and increasing the relevance of OH chemistry. Ozone–alkene reactions may also lead to high  $[\text{OH}]_{\text{ss}}$  when ventilation rates are high. This could lead to processes such as particle formation and oxidation of species associated with interior materials such as brominated flame retardants. We suggest that oxidative capacity should be considered when investigating IAQ in vehicles.

## Data availability

The data collected in this study are available on request from the corresponding author, Dr Tara F. Kahan.



## Conflicts of interest

There are no conflicts to declare.

## Acknowledgements

Funding for this work was provided by the Alfred P. Sloan Foundation CIE program (G-2018-11062). Dr Kahan is a Canada Research Chair in Environmental Analytical Chemistry. This work was undertaken, in part, thanks to funding from the Canada Research Chairs program. PAFS acknowledges Saskatchewan Innovation and Opportunity Scholarship for the scholarship granted.

## References

- 1 N. E. Klepeis, W. C. Nelson, W. R. Ott, J. P. Robinson, A. M. Tsang, P. Switzer, J. V. Behar, S. C. Hern and W. H. Engelmann, The National Human Activity Pattern Survey (NHAPS): A Resource for Assessing Exposure to Environmental Pollutants, *J. Exposure Sci. Environ. Epidemiol.*, 2001, **11**(3), 231–252, DOI: [10.1038/sj.jea.7500165](https://doi.org/10.1038/sj.jea.7500165).
- 2 L. Abi-Esber and M. El-Fadel, Indoor to Outdoor Air Quality Associations with Self-Pollution Implications inside Passenger Car Cabins, *Atmos. Environ.*, 2013, **81**, 450–463, DOI: [10.1016/j.atmosenv.2013.09.040](https://doi.org/10.1016/j.atmosenv.2013.09.040).
- 3 A. Leavey, N. Reed, S. Patel, K. Bradley, P. Kulkarni and P. Biswas, Comparing On-Road Real-Time Simultaneous in-Cabin and Outdoor Particulate and Gaseous Concentrations for a Range of Ventilation Scenarios, *Atmos. Environ.*, 2017, **166**, 130–141, DOI: [10.1016/j.atmosenv.2017.07.016](https://doi.org/10.1016/j.atmosenv.2017.07.016).
- 4 J. Dröge, R. Müller, C. Scutaru, M. Braun and D. Groneberg, Mobile Measurements of Particulate Matter in a Car Cabin: Local Variations, Contrasting Data from Mobile *versus* Stationary Measurements and the Effect of an Opened *versus* a Closed Window, *Int. J. Environ. Res. Public Health*, 2018, **15**(12), 2642, DOI: [10.3390/ijerph15122642](https://doi.org/10.3390/ijerph15122642).
- 5 T. Moreno, A. Pacitto, A. Fernández, F. Amato, E. Marco, J. O. Grimalt, G. Buonanno and X. Querol, Vehicle Interior Air Quality Conditions When Travelling by Taxi, *Environ. Res.*, 2019, **172**, 529–542, DOI: [10.1016/j.envres.2019.02.042](https://doi.org/10.1016/j.envres.2019.02.042).
- 6 E. I. Tolis, T. Karanotas, G. Svolakis, G. Panaras and J. G. Bartzis, Air Quality in Cabin Environment of Different Passenger Cars: Effect of Car Usage, Fuel Type and Ventilation/Infiltration Conditions, *Environ. Sci. Pollut. Res.*, 2021, **28**(37), 51232–51241, DOI: [10.1007/s11356-021-14349-9](https://doi.org/10.1007/s11356-021-14349-9).
- 7 L. Pitten, D. Brüggemann, J. Dröge, M. Braun and D. A. Groneberg, Impact of Different Ventilation Conditions on Tobacco Smoke-Associated Particulate Matter Emissions in a Car Cabin Using the TAPaC Platform, *Sci. Rep.*, 2023, **13**(1), 8216, DOI: [10.1038/s41598-023-35208-2](https://doi.org/10.1038/s41598-023-35208-2).
- 8 C. J. Weschler, M. Brauer and P. Koutrakis, Indoor Ozone and Nitrogen Dioxide: A Potential Pathway to the Generation of Nitrate Radicals, Dinitrogen Pentoxide, and Nitric Acid Indoors, *Environ. Sci. Technol.*, 1992, **26**(1), 179–184, DOI: [10.1021/es00025a022](https://doi.org/10.1021/es00025a022).
- 9 J. K. Nøjgaard, Indoor Measurements of the Sum of the Nitrate Radical,  $\text{NO}_3$ , and Nitrogen Pentoxide,  $\text{N}_2\text{O}_5$  in Denmark, *Chemosphere*, 2010, **79**(8), 898–904, DOI: [10.1016/j.chemosphere.2010.02.025](https://doi.org/10.1016/j.chemosphere.2010.02.025).
- 10 C. Arata, K. J. Zarzana, P. K. Misztal, Y. Liu, S. S. Brown, W. W. Nazaroff and A. H. Goldstein, Measurement of  $\text{NO}_3$  and  $\text{N}_2\text{O}_5$  in a Residential Kitchen, *Environ. Sci. Technol. Lett.*, 2018, **5**(10), 595–599, DOI: [10.1021/acs.estlett.8b00415](https://doi.org/10.1021/acs.estlett.8b00415).
- 11 A. Moravek, T. C. VandenBoer, Z. Finewax, D. Pagonis, B. A. Nault, W. L. Brown, D. A. Day, A. V. Handschy, H. Stark, P. Ziemann, J. L. Jimenez, J. A. De Gouw and C. J. Young, Reactive Chlorine Emissions from Cleaning and Reactive Nitrogen Chemistry in an Indoor Athletic Facility, *Environ. Sci. Technol.*, 2022, **56**(22), 15408–15416, DOI: [10.1021/acs.est.2c04622](https://doi.org/10.1021/acs.est.2c04622).
- 12 S. Uchiyama, T. Tomizawa, A. Tokoro, M. Aoki, M. Hishiki, T. Yamada, R. Tanaka, H. Sakamoto, T. Yoshida, K. Bekki, Y. Inaba, H. Nakagome and N. Kunugita, Gaseous Chemical Compounds in Indoor and Outdoor Air of 602 Houses throughout Japan in Winter and Summer, *Environ. Res.*, 2015, **137**, 364–372, DOI: [10.1016/j.envres.2014.12.005](https://doi.org/10.1016/j.envres.2014.12.005).
- 13 C. J. Weschler, Ozone in Indoor Environments: Concentration and Chemistry: Ozone in Indoor Environments, *Indoor Air*, 2000, **10**(4), 269–288, DOI: [10.1034/j.1600-0668.2000.010004269.x](https://doi.org/10.1034/j.1600-0668.2000.010004269.x).
- 14 S. Gligorovski, R. Strekowski, S. Barbat and D. Vione, Environmental Implications of Hydroxyl Radicals ( $\cdot\text{OH}$ ), *Chem. Rev.*, 2015, **115**(24), 13051–13092, DOI: [10.1021/cr500310b](https://doi.org/10.1021/cr500310b).
- 15 E. Gomez Alvarez, D. Amedro, C. Afif, S. Gligorovski, C. Schoemaecker, C. Fittschen, J.-F. Doussin and H. Wortham, Unexpectedly High Indoor Hydroxyl Radical Concentrations Associated with Nitrous Acid, *Proc. Natl. Acad. Sci. U. S. A.*, 2013, **110**(33), 13294–13299, DOI: [10.1073/pnas.1308310110](https://doi.org/10.1073/pnas.1308310110).
- 16 N. Carslaw, L. Fletcher, D. Heard, T. Ingham and H. Walker, Significant OH Production under Surface Cleaning and Air Cleaning Conditions: Impact on Indoor Air Quality, *Indoor Air*, 2017, **27**(6), 1091–1100, DOI: [10.1111/ina.12394](https://doi.org/10.1111/ina.12394).
- 17 D. Stone, L. K. Whalley and D. E. Heard, Tropospheric OH and  $\text{HO}_2$  Radicals: Field Measurements and Model Comparisons, *Chem. Soc. Rev.*, 2012, **41**(19), 6348, DOI: [10.1039/c2cs35140d](https://doi.org/10.1039/c2cs35140d).
- 18 S. F. Kowal, S. R. Allen and T. F. Kahan, Wavelength-Resolved Photon Fluxes of Indoor Light Sources: Implications for  $\text{HO}_x$  Production, *Environ. Sci. Technol.*, 2017, **51**(18), 10423–10430, DOI: [10.1021/acs.est.7b02015](https://doi.org/10.1021/acs.est.7b02015).
- 19 J. Stutz, E. S. Kim, U. Platt, P. Bruno, C. Perrino and A. Febo, UV-Visible Absorption Cross Sections of Nitrous Acid, *J. Geophys. Res.: Atmos.*, 2000, **105**(D11), 14585–14592, DOI: [10.1029/2000JD900003](https://doi.org/10.1029/2000JD900003).
- 20 J. B. Burkholder, S. P. Sander, J. P. D. Abbatt, J. R. Barker, C. Cappa, J. D. Crounse, T. S. Dibble, R. E. Huie, C. E. Kolb, M. J. Kurylo, V. L. Orkin, C. J. Percival,



D. M. Wilmouth and P. H. Wine *Chemical Kinetics and Photochemical Data for Use in Atmospheric Studies, Evaluation No. 19; JPL Publication 19-5*, California Institute of Technology: Jet Propulsion Laboratory, Pasadena, 2019, <https://jpldataeval.jpl.nasa.gov/>.

21 K. J. Wall, C. L. Schiller and G. W. Harris, Measurements of the HONO Photodissociation Constant, *J. Atmos. Chem.*, 2006, **55**(1), 31–54, DOI: [10.1007/s10874-006-9021-2](https://doi.org/10.1007/s10874-006-9021-2).

22 M. Mendez, D. Amedro, N. Blond, D. A. Hauglustaine, P. Blondeau, C. Afif, C. Fittschen and C. Schoemaeker, Identification of the Major HO<sub>x</sub> Radical Pathways in an Indoor Air Environment, *Indoor Air*, 2017, **27**(2), 434–442, DOI: [10.1111/ina.12316](https://doi.org/10.1111/ina.12316).

23 S. Zhou, S. F. Kowal, A. R. Cregan and T. F. Kahan, Factors Affecting Wavelength-Resolved Ultraviolet Irradiance Indoors and Their Impacts on Indoor Photochemistry, *Indoor Air*, 2020, **31**(4), 1187–1198, DOI: [10.1111/ina.12784](https://doi.org/10.1111/ina.12784).

24 S. Zhou and T. F. Kahan, Spatiotemporal Characterization of Irradiance and Photolysis Rate Constants of Indoor Gas-Phase Species in the UTest House during HOMEChem, *Indoor Air*, 2022, **32**(1), e12964, DOI: [10.1111/ina.12966](https://doi.org/10.1111/ina.12966).

25 Y. Won, M. Waring and D. Rim, Understanding the Spatial Heterogeneity of Indoor OH and HO<sub>2</sub> Due to Photolysis of HONO Using Computational Fluid Dynamics Simulation, *Environ. Sci. Technol.*, 2019, **53**(24), 14470–14478, DOI: [10.1021/acs.est.9b06315](https://doi.org/10.1021/acs.est.9b06315).

26 T. F. Kahan, C. J. Young and S. Zhou, *Indoor Photochemistry*, in *Handbook of Indoor Air Quality*, Zhang Y., Hopke P. K. and Mandin C., Springer Singapore, Singapore, 2022; pp. 1–30, DOI: [10.1007/978-981-10-5155-5\\_30-1](https://doi.org/10.1007/978-981-10-5155-5_30-1).

27 M. Riediker, R. Williams, R. Devlin, T. Griggs and P. Bromberg, Exposure to Particulate Matter, Volatile Organic Compounds, and Other Air Pollutants Inside Patrol Cars, *Environ. Sci. Technol.*, 2003, **37**(10), 2084–2093, DOI: [10.1021/es026264y](https://doi.org/10.1021/es026264y).

28 A. Febo and C. Perrino, Measurement of High Concentration of Nitrous Acid inside Automobiles, *Atmos. Environ.*, 1995, **29**(3), 345–351, DOI: [10.1016/1352-2310\(94\)00260-R](https://doi.org/10.1016/1352-2310(94)00260-R).

29 S. Zhou, C. J. Young, T. C. VandenBoer, S. F. Kowal and T. F. Kahan, Time-Resolved Measurements of Nitric Oxide, Nitrogen Dioxide, and Nitrous Acid in an Occupied New York Home, *Environ. Sci. Technol.*, 2018, **52**(15), 8355–8364, DOI: [10.1021/acs.est.8b01792](https://doi.org/10.1021/acs.est.8b01792).

30 C. W. Spicer, D. V. Kenny, G. F. Ward, I. H. Billick and N. P. Leslie, Evaluation of NO<sub>2</sub> Measurement Methods for Indoor Air Quality Applications, *Air Waste*, 1994, **44**(2), 163–168, DOI: [10.1080/1073161X.1994.10467245](https://doi.org/10.1080/1073161X.1994.10467245).

31 C. J. Young, S. Zhou, J. A. Siegel and T. F. Kahan, Illuminating the Dark Side of Indoor Oxidants, *Environ. Sci.: Processes Impacts*, 2019, **21**(8), 1229–1239, DOI: [10.1039/C9EM00111E](https://doi.org/10.1039/C9EM00111E).

32 S. Zhou, C. J. Young, T. C. VandenBoer and T. F. Kahan, Role of Location, Season, Occupant Activity, and Chemistry in Indoor Ozone and Nitrogen Oxide Mixing Ratios, *Environ. Sci.: Processes Impacts*, 2019, **21**(8), 1374–1383, DOI: [10.1039/C9EM00129H](https://doi.org/10.1039/C9EM00129H).

33 W. W. Nazaroff and C. J. Weschler, Indoor Ozone: Concentrations and Influencing Factors, *Indoor Air*, 2022, **32**(1), 1–21, DOI: [10.1111/ina.12942](https://doi.org/10.1111/ina.12942).

34 L. D. Knibbs, R. J. de Dear and S. E. Atkinson, Field Study of Air Change and Flow Rate in Six Automobiles, *Indoor Air*, 2009, **19**(4), 303–313, DOI: [10.1111/j.1600-0668.2009.00593.x](https://doi.org/10.1111/j.1600-0668.2009.00593.x).

35 N. Hudda, E. Kostenidou, C. Sioutas, R. J. Delfino and S. A. Fruin, Vehicle and Driving Characteristics That Influence In-Cabin Particle Number Concentrations, *Environ. Sci. Technol.*, 2011, **45**(20), 8691–8697, DOI: [10.1021/es202025m](https://doi.org/10.1021/es202025m).

36 W. W. Nazaroff, Residential Air-change Rates: A Critical Review, *Indoor Air*, 2021, **31**(2), 282–313, DOI: [10.1111/ina.12785](https://doi.org/10.1111/ina.12785).

37 J. H. Park, J. D. Spengler, D. W. Yoon, T. Dumyahn, K. Lee and H. Ozkaynak, Measurement of Air Exchange Rate of Stationary Vehicles and Estimation of In-Vehicle Exposure, *J. Exposure Anal. Environ. Epidemiol.*, 1998, **8**(1), 65–78.

38 B. P. Leaderer, L. Naeher, T. Jankun, K. Balenger, C. Toth, J. M. Wolfson and P. Kourakis, Indoor, Outdoor, and Regional Summer and Winter Concentrations of PM<sub>2.5</sub>, S<sub>42-</sub>, H<sup>+</sup>, NH<sub>4</sub><sup>+</sup>, NO<sub>3</sub><sup>-</sup>, NH<sub>3</sub>, and Nitrous Acid in Homes with and without Kerosene Space Heaters, *Environ. Health Perspect.*, 1999, **107**(3), 223–231, DOI: [10.1289/ehp.99107223](https://doi.org/10.1289/ehp.99107223).

39 B. J. Finlayson-Pitts, L. M. Wingen, A. L. Sumner, D. Syomin and K. A. Ramazan, The Heterogeneous Hydrolysis of NO<sub>2</sub> in Laboratory Systems and in Outdoor and Indoor Atmospheres: An Integrated Mechanism, *Phys. Chem. Chem. Phys.*, 2003, **5**(2), 223–242, DOI: [10.1039/B208564J](https://doi.org/10.1039/B208564J).

40 E. L. Avol, W. C. Navidi and S. D. Colome, Modeling Ozone Levels in and around Southern California Homes, *Environ. Sci. Technol.*, 1998, **32**(4), 463–468, DOI: [10.1021/es970351m](https://doi.org/10.1021/es970351m).

41 E. Gómez Alvarez, H. Wortham, R. Strelkowski, C. Zetzs and S. Gligorovski, Atmospheric Photosensitized Heterogeneous and Multiphase Reactions: From Outdoors to Indoors, *Environ. Sci. Technol.*, 2012, **46**(4), 1955–1963, DOI: [10.1021/es2019675](https://doi.org/10.1021/es2019675).

42 E. Reidy, B. P. Bottorff, C. M. F. Rosales, F. J. Cardoso-Saldaña, C. Arata, S. Zhou, C. Wang, A. Abeleira, L. Hildebrandt Ruiz, A. H. Goldstein, A. Novoselac, T. F. Kahan, J. P. D. Abbatt, M. E. Vance, D. K. Farmer and P. S. Stevens, Measurements of Hydroxyl Radical Concentrations during Indoor Cooking Events: Evidence of an Unmeasured Photolytic Source of Radicals, *Environ. Sci. Technol.*, 2023, **57**(2), 896–908, DOI: [10.1021/acs.est.2c05756](https://doi.org/10.1021/acs.est.2c05756).

43 C. Tuchinda, S. Srivannaboon and H. W. Lim, Photoprotection by Window Glass, Automobile Glass, and Sunglasses, *J. Am. Acad. Dermatol.*, 2006, **54**(5), 845–854, DOI: [10.1016/j.jaad.2005.11.1082](https://doi.org/10.1016/j.jaad.2005.11.1082).

44 K. Lee, J. Xue, A. S. Geyh, H. Ozkaynak, B. P. Leaderer, C. J. Weschler and J. D. Spengler, Nitrous Acid, Nitrogen Dioxide, and Ozone Concentrations in Residential Environments, *Environ. Health Perspect.*, 2002, **110**(2), 145–150, DOI: [10.1289/ehp.0211045](https://doi.org/10.1289/ehp.0211045).



45 D. B. Collins, R. F. Hems, S. Zhou, C. Wang, E. Grignon, M. Alavy, J. A. Siegel and J. P. D. Abbatt, Evidence for Gas-Surface Equilibrium Control of Indoor Nitrous Acid, *Environ. Sci. Technol.*, 2018, **52**(21), 12419–12427, DOI: [10.1021/acs.est.8b04512](https://doi.org/10.1021/acs.est.8b04512).

46 H. Deng, X. Xu, K. Wang, J. Xu, G. Loisel, Y. Wang, H. Pang, P. Li, Z. Mai, S. Yan, X. Li and S. Gligorovski, The Effect of Human Occupancy on Indoor Air Quality through Real-Time Measurements of Key Pollutants, *Environ. Sci. Technol.*, 2022, **56**(22), 15377–15388, DOI: [10.1021/acs.est.2c04609](https://doi.org/10.1021/acs.est.2c04609).

47 D. K. Farmer, M. E. Vance, J. P. D. Abbatt, A. Abeleira, M. R. Alves, C. Arata, E. Boedicker, S. Bourne, F. Cardoso-Saldaña, R. Corsi, P. F. DeCarlo, A. H. Goldstein, V. H. Grassian, L. Hildebrandt Ruiz, J. L. Jimenez, T. F. Kahan, E. F. Katz, J. M. Mattila, W. W. Naszaroff, A. Novoselac, R. E. O'Brien, V. W. Or, S. Patel, S. Sankhyan, P. S. Stevens, Y. Tian, M. Wade, C. Wang, S. Zhou and Y. Zhou, Overview of HOMECHEM: House Observations of Microbial and Environmental Chemistry, *Environ. Sci.: Processes Impacts*, 2019, **21**(8), 1280–1300, DOI: [10.1039/C9EM00228F](https://doi.org/10.1039/C9EM00228F).

48 J. Liu, S. Li, J. Zeng, M. Mekic, Z. Yu, W. Zhou, G. Loisel, A. Gandolfo, W. Song, X. Wang, Z. Zhou, H. Herrmann, X. Li and S. Gligorovski, Assessing Indoor Gas Phase Oxidation Capacity through Real-Time Measurements of HONO and NO<sub>x</sub> in Guangzhou, China, *Environ. Sci.: Processes Impacts*, 2019, **21**(8), 1393–1402, DOI: [10.1039/C9EM00194H](https://doi.org/10.1039/C9EM00194H).

49 S. S. Park, J. H. Hong, J. H. Lee, Y. J. Kim, S. Y. Cho and S. J. Kim, Investigation of Nitrous Acid Concentration in an Indoor Environment Using an In-Situ Monitoring System, *Atmos. Environ.*, 2008, **42**(27), 6586–6596, DOI: [10.1016/j.atmosenv.2008.05.023](https://doi.org/10.1016/j.atmosenv.2008.05.023).

50 M. Blocquet, F. Guo, M. Mendez, M. Ward, S. Coudert, S. Batut, C. Hecquet, N. Blond, C. Fittschen and C. Schoemaeker, Impact of the Spectral and Spatial Properties of Natural Light on Indoor Gas-Phase Chemistry: Experimental and Modeling Study, *Indoor Air*, 2018, **28**(3), 426–440, DOI: [10.1111/ina.12450](https://doi.org/10.1111/ina.12450).

51 A. Gandolfo, V. Gligorovski, V. Bartolomei, S. Tlili, E. Gómez Alvarez, H. Wortham, J. Kleffmann and S. Gligorovski, Spectrally Resolved Actinic Flux and Photolysis Frequencies of Key Species within an Indoor Environment, *Build. Sci.*, 2016, **109**, 50–57, DOI: [10.1016/j.buildenv.2016.08.026](https://doi.org/10.1016/j.buildenv.2016.08.026).

52 S. E. Pusede, T. C. VandenBoer, J. G. Murphy, M. Z. Markovic, C. J. Young, P. R. Veres, J. M. Roberts, R. A. Washenfelder, S. S. Brown, X. Ren, C. Tsai, J. Stutz, W. H. Brune, E. C. Browne, P. J. Wooldridge, A. R. Graham, R. Weber, A. H. Goldstein, S. Dusanter, S. M. Griffith, P. S. Stevens, B. L. Lefer and R. C. Cohen, An Atmospheric Constraint on the NO<sub>2</sub> Dependence of Daytime Near-Surface Nitrous Acid (HONO), *Environ. Sci. Technol.*, 2015, **49**(21), 12774–12781, DOI: [10.1021/acs.est.5b02511](https://doi.org/10.1021/acs.est.5b02511).

53 B. Bottorff, E. Reidy, L. Mielke, S. Dusanter and P. S. Stevens, Development of a Laser-Photofragmentation Laser-Induced Fluorescence Instrument for the Detection of Nitrous Acid and Hydroxyl Radicals in the Atmosphere, *Atmos. Meas. Tech.*, 2021, **14**(9), 6039–6056, DOI: [10.5194/amt-14-6039-2021](https://doi.org/10.5194/amt-14-6039-2021).

54 A. Besis, T. Katsaros and C. Samara, Concentrations of Volatile Organic Compounds in Vehicular Cabin Air – Implications to Commuter Exposure, *Environ. Pollut.*, 2023, **330**, 121763, DOI: [10.1016/j.envpol.2023.121763](https://doi.org/10.1016/j.envpol.2023.121763).

55 P. Neeb and G. K. Moortgat, Formation of OH Radicals in the Gas-Phase Reaction of Propene, Isobutene, and Isoprene with O<sub>3</sub> : Yields and Mechanistic Implications, *J. Phys. Chem. A*, 1999, **103**(45), 9003–9012, DOI: [10.1021/jp9903458](https://doi.org/10.1021/jp9903458).

56 V. G. Khamaganov and R. A. Hites, Rate Constants for the Gas-Phase Reactions of Ozone with Isoprene,  $\alpha$ - and  $\beta$ -Pinene, and Limonene as a Function of Temperature, *J. Phys. Chem. A*, 2001, **105**(5), 815–822, DOI: [10.1021/jp002730z](https://doi.org/10.1021/jp002730z).

57 M. S. Waring and J. R. Wells, Volatile Organic Compound Conversion by Ozone, Hydroxyl Radicals, and Nitrate Radicals in Residential Indoor Air: Magnitudes and Impacts of Oxidant Sources, *Atmos. Environ.*, 2015, **106**, 382–391, DOI: [10.1016/j.atmosenv.2014.06.062](https://doi.org/10.1016/j.atmosenv.2014.06.062).

58 M. F. Link, J. Li, J. C. Ditto, H. Huynh, J. Yu, S. M. Zimmerman, K. L. Rediger, A. Shore, J. P. D. Abbatt, L. A. Garofalo, D. K. Farmer and D. Poppendieck, Ventilation in a Residential Building Brings Outdoor NO<sub>x</sub> Indoors with Limited Implications for VOC Oxidation from NO<sub>3</sub> Radicals, *Environ. Sci. Technol.*, 2023, **57**(43), 16446–16455, DOI: [10.1021/acs.est.3c04816](https://doi.org/10.1021/acs.est.3c04816).

